Geophysical Research Letters

RESEARCH LETTER
10.1029/2018GL081574

Key Points:
- Drag coefficients under five different tropical cyclones
- New data-based parameterization of drag coefficients using surface wave effects

Supporting Information:
- Supporting Information S1

Correspondence to:
J.-Y. Hsu,
je-yuan.hsu@csiro.au

Citation:
Hsu, J.-Y., Lien, R.-C., D'Asaro, E. A., & Sanford, T. B. (2019). Scaling of drag coefficients under five tropical cyclones. *Geophysical Research Letters*, *46*. https://doi.org/10.1029/2018GL081574

Received 3 DEC 2018
Accepted 27 FEB 2019
Accepted article online 4 MAR 2019

Scaling of Drag Coefficients Under Five Tropical Cyclones

Je-Yuan Hsu[1], Ren-Chieh Lien[2], Eric A. D'Asaro[2], and Thomas B. Sanford[2]

[1]Commonwealth Scientific and Industrial Research Organisation, Perth, Australia, [2]Applied Physics Laboratory, University of Washington, Seattle, WA, USA

Abstract The drag coefficient, often used to parameterize the surface wind stress $\boldsymbol{\tau}$, beneath tropical cyclones (TCs) is a critical but poorly known factor controlling TC intensity. Here, $\boldsymbol{\tau}$ is estimated using current measurements taken by 12 Electromagnetic Autonomous Profiling Explorer floats beneath the forward half of five TCs. Combining estimates of $\boldsymbol{\tau}$ and aircraft measurements of winds $\mathbf{U_{10}}$, the downwind drag coefficient $\widetilde{C_{\parallel}}$ and the angle ϕ clockwise orientation from $\mathbf{U_{10}}$ to $\boldsymbol{\tau}$ are computed. At $|\mathbf{U_{10}}| = 25$–40 m/s, $\widetilde{C_{\parallel}}$ and ϕ vary over $(0.8$–$3.1) \times 10^{-3}$ and -15–$40°$, respectively. A new nondimensional parameter "effective wind duration," a function of $|\mathbf{U_{10}}|$, storm translation speed, and positions in TCs, predicts $\widetilde{C_{\parallel}}$ to within 25%. The largest $\widetilde{C_{\parallel}}$ and smallest ϕ occur at high winds, in the forward right quadrant of fast-moving storms. These dependences are explained by variations in surface wave age and breaking under different wave forcing regimes.

Plain Language Summary The forecast of tropical cyclone intensification is critical to the protection of coastlines, involving the complicated tropical cyclone-ocean interaction. The wind of storms can force strong near-inertial current via surface wind stress (often parameterized by a drag coefficient C_d), and then induce the upper ocean cooling due to the shear instability. The transferred momentum and reduced heat supply can both restrict tropical cyclones' development. In other words, the C_d can affect the prediction of momentum and thermal response under storms, and thereby the forecast on storm intensity. This study investigates the spatial variability of downwind drag coefficient C_d under five different tropical cyclones, by integrating the storm-induced ocean momentum because previous results of C_d as a function of wind speed $|\mathbf{U_{10}}|$ are scattered significantly at $|\mathbf{U_{10}}|$=25-40 m/s. Here, larger C_d in the front-right sector of faster storms than that of slower stoms is found, presumably due to the surface wave effect. A new parameterization of C_d using the surface wave properties under tropical cyclones is proposed, which largely improves the conventional parameterization of $C_d(|\mathbf{U_{10}}|)$. Future studies on the tropical cyclone-wave-ocean interaction and storm intensification forecast will be benefited from this new parameterization.

1. Introduction

Surface wind stress $\boldsymbol{\tau}$ of tropical cyclones (TCs) acts as a major forcing to upper ocean dynamics, for example, near-inertial current, which may trigger shear instability and lead to strong vertical mixing and surface mixed layer cooling on the right side of storm tracks (Price et al., 1994). Both the momentum transfer into the ocean via $\boldsymbol{\tau}$, and the induced upper ocean cooling can affect the intensification of tropical cyclones (Balaguru et al., 2015; Emanuel, 1995). The $\boldsymbol{\tau}$ in tropical cyclone has been studied extensively in the laboratory (e.g., Donelan et al., 2004; Takagaki et al., 2012) or field experiments (Hsu et al., 2017; Powell et al., 2003; Sanford et al., 2011), and is often parameterized by a drag coefficient C_d as $|\boldsymbol{\tau}| = \rho_{\mathrm{air}} C_d |\mathbf{U_{10}}|^2$, where ρ_{air} is the air density, and $\mathbf{U_{10}}$ the wind at 10-m height above sea surface.

Many previous studies conclude that C_d increases linearly with wind speed at $|\mathbf{U_{10}}| < 20$ m/s (Edson et al., 2013; Large & Pond, 1981) and remains constant at 1.5–2.0×10^{-3} at $|\mathbf{U_{10}}| > 40$ m/s (Hsu et al., 2017; Powell et al., 2003; Sanford et al., 2011). At $|\mathbf{U_{10}}| = 25$–40 m/s, the values of C_d widely range from 1.5 to 4.5×10^{-3} (Bryant & Akbar, 2016; Donelan et al., 2004; Holthuijsen et al., 2012; Hsu et al., 2017; Jarosz et al., 2007; Powell et al., 2003; Sanford et al., 2011), presumably because factors other than wind speed are important, such as the spatial variability of surface gravity waves (Holthuijsen et al., 2012). Several studies use atmosphere-wave-ocean coupling models (Chen et al., 2013; Reichl et al., 2014) to simulate the map of C_d under tropical cyclones. The simulated C_d in the front-right quadrant of tropical cyclones is higher than that in the front-left quadrant, inconsistent with the spatial pattern observed by Holthuijsen et al. (2012). The $\boldsymbol{\tau}$ has also been reported to be misaligned with $\mathbf{U_{10}}$ under tropical cyclones

(Hsu et al., 2017; Potter et al., 2015), presumably due to the influence of surface wave propagation (Potter et al., 2015).

Jarosz et al. (2007) and Sanford et al. (2011) estimate the surface wind stress under hurricanes, assuming a linear momentum budget, using the measurements of storm-induced ocean current velocity. Hsu et al. (2017) apply the same method under Typhoon Megi 2010 and carefully remove effects of background currents on surface wind stress estimates. Here, we extend the analysis to explore the variability of drag coefficients in five tropical cyclones (section 5). These data are used to develop a new parameterization which includes the effects of surface waves (section 6), in addition to $|\mathbf{U_{10}}|$.

2. Experiments in Tropical Cyclones

As a part of the 2004 Coupled Boundary Layer Air-Sea Transfer Experiment (CBLAST) (Black et al., 2007) and 2010 Impact of Typhoons on the Ocean in the Pacific (ITOP) programs (D'Asaro et al., 2014), a series of experiments were conducted in tropical cyclones, including Frances 2004, Gustav 2008 (Rabe et al., 2015), Ike 2008, Fanapi 2010, and Megi 2010 (Figure 1). Nineteen Electromagnetic Autonomous Profiling Explorer (EM-APEX) floats were air-launched by aircraft ~1 day before four tropical cyclones, except Ike. A total of 668 air-dropsondes measuring wind, temperature, and humidity profiles were deployed in these storms as they passed over the floats. These were processed by the National Center for Atmospheric Research/Earth Observing Laboratory. Stepped-Frequency Microwave Radiometers mounted on the aircraft measured brightness temperature which was used to estimate $|\mathbf{U_{10}}|$. For Fanapi and Megi, the dropsondes and microwave measurements were combined to create maps of $|\mathbf{U_{10}}|$ as described in the supporting information A. Wind fields for Frances, Gustav, and Ike were provided by Atlantic Oceanographic and Meteorological Laboratory/Hurricane Research Division/National Oceanic and Atmospheric Administration (AOML/HRD/NOAA). The wind maps used are shown in Figure 1. Estimates of $\mathbf{U_{10}}$ at float positions are interpolated using the observed wind maps.

Megi has the smallest radius of maximum wind speed ($R_{\max}$ = 14 km), the fastest translation speed (U_h = 7.7 m/s), and the greatest maximum wind speed ($V_{\max}$ = 75 m/s) (supporting information B). Gustav has similar $V_{\max}$ (46 m/s) with Fanapi (52 m/s), but larger $R_{\max}$ (46 km > 20 km) and faster U_h (7.7 m/s > 3.8 m/s). Ike has the largest $R_{\max}$ (75 km) but the lowest $V_{\max}$ (41 m/s) of the five tropical cyclones. Frances has the greater $V_{\max}$ (56 m/s), with $R_{\max}$ (30 km) smaller than Gustav and Ike.

3. EM-APEX Float Measurements

EM-APEX floats measured vertical profiles of horizontal current velocity, temperature and salinity (Sanford et al., 2005). The vertical profiling speed was ~ 0.11 m/s, resulting ~3-m vertical resolution of current velocity due to the data processing in every 50-s data window with 25-s overlap. During Frances and Megi, floats did not profile shallower than 30-m depth, to avoid damage by storm-induced ocean surface waves (Hsu et al., 2017; Sanford et al., 2011). Missing measurements in the upper 30 m were extrapolated using the uppermost velocity measurements in each profile. The effect of extrapolated current velocity to the drag coefficient results is negligible (supporting information C). Twelve floats captured the oceanic response to winds greater than 25 m/s (supporting information B). Seven floats passed the right-hand side of tropical cyclones' track, three floats passed the eyes of Frances, Fanapi, and Megi, and two floats passed the left-hand side of Gustav and Fanapi's tracks. The float deployed on the left side of Gustav's track drifted to the right side of Ike's track.

4. Method of Estimating Drag Coefficients

Sanford et al. (2011) and Hsu et al. (2017) estimate the surface wind stress $\widetilde{\boldsymbol{\tau}}$ using float measurements of horizontal current velocity $\mathbf{v}$, assuming surface wind stress $\boldsymbol{\tau}$ balanced with the acceleration of ocean current velocity $\partial\mathbf{v}/\partial t$ and Coriolis force $f\widehat{\mathbf{k}}\times\mathbf{v}$ in the linear momentum budget, that is,

$$\widetilde{\boldsymbol{\tau}} = \boldsymbol{\tau} + \Delta\boldsymbol{\tau} = \rho_0\int_{-H}^{0}\left(\frac{\partial\mathbf{v}}{\partial t} + f\widehat{\mathbf{k}}\times\mathbf{v}\right)dz \quad (1)$$

where $\Delta\boldsymbol{\tau}$ is the uncertainty of $\widetilde{\boldsymbol{\tau}}$, $\mathbf{v} = u\widehat{\mathbf{i}} + v\widehat{\mathbf{j}}$, $\widehat{\mathbf{i}}$ and $\widehat{\mathbf{j}}$ the unit vectors in east and north directions, respectively, H = 100 m the base of momentum integration in this study, f the local Coriolis frequency, ρ_0 the Boussinesq

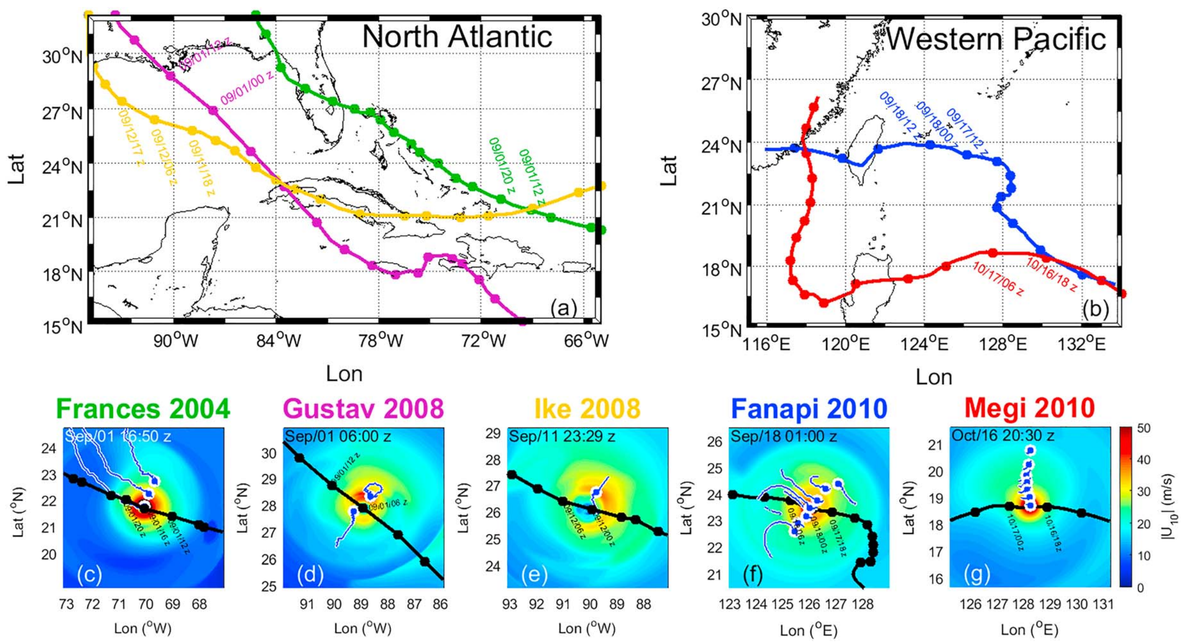

Figure 1. The tracks of hurricanes in the North Atlantic (a), Frances: green; Gustav: purple; Ike: gold. The tracks of typhoons in the western Pacific (b), Fanapi: blue; Megi: red. Tropical cyclone wind maps at the time eyes pass near EM-APEX float positions (c–g) and trajectories of float positions (blue dots connected with lines in c–g). The colored dots connected with thick lines in (a) and (b) are tracks of tropical cyclone eyes every 12 hr, and the black dots connected with a thick line in (c)–(g) are tracks of tropical cyclone eyes every 6 hr.

density, and $\widehat{\mathbf{k}}$ vertical unit vector. The vector $\boldsymbol{\tau}$ is represented in the cross-wind and along-wind components (Hsu et al., 2017) as

$$\boldsymbol{\tau} = \tau_{\perp}\widehat{\mathbf{U_{10}}}_{\perp}+\tau_{\parallel}\widehat{\mathbf{U_{10}}}_{\parallel} \text{ and } \phi = \tan^{-1}\frac{\tau_{\perp}}{\tau_{\parallel}} \tag{2}$$

where $\widehat{\mathbf{U_{10}}}_{\perp}$ and $\widehat{\mathbf{U_{10}}}_{\parallel}$ are unit vectors perpendicular and along the $\mathbf{U_{10}}$ (Figure 2c), $\tau_{\perp}$ and $\tau_{\parallel}$ the projected stress at the crosswind and downwind directions, respectively, and ϕ the angle between the surface wind stress $\boldsymbol{\tau}$ and $\mathbf{U_{10}}$ rotating clockwisely from $\mathbf{U_{10}}$ to $\boldsymbol{\tau}$. Note that $\tau_{\perp} > 0$ and $\phi > 0$ when $\boldsymbol{\tau}$ is clockwise from $\mathbf{U_{10}}$. Crosswind $C_{\perp}$ and downwind drag coefficients $C_{\parallel}$ are parameterized as

$$C_{\perp} = \frac{\tau_{\perp}}{\rho_{\text{air}}|\mathbf{U_{10}}|^2} \text{ and } C_{\parallel} = \frac{\tau_{\parallel}}{\rho_{\text{air}}|\mathbf{U_{10}}|^2} \tag{3}$$

Previous studies (e.g., Powell et al., 2003) often report the estimates of drag coefficient C_d assuming the alignment between $\boldsymbol{\tau}$ and $\mathbf{U_{10}}$, that is, the $C_{\parallel}$ is the same as the conventional definition of C_d. The $C_{\parallel}$ and $C_{\perp}$ are the drag coefficients "felt" by the ocean current under the storms (i.e., Reynolds flux from the atmosphere into the ocean), and may differ to the C_d estimated using the wind measurements (i.e., Reynolds flux in the atmosphere; Jones & Toba, 2012). Nonlinearities in the ocean response limit the use of this method (equation (1)) to the forward half of the storm (Hsu et al., 2017), that is, before the storm eye passes the floats. Thus, all of the results presented here are limited to the front part of the storm.

Ocean current not forced by tropical cyclone wind, such as tides and eddies, may result in errors on estimates of surface wind stress using equation (1) (Hsu et al., 2017) and are removed from velocity measurements (supporting information B). Effects of horizontal advection, divergence, and pressure gradient terms excluded in equation (1) are corrected using results from a PWP3D model (Price et al., 1994) (supporting information C). Downwind drag coefficients $\widetilde{C_{\parallel}}$ and angles ϕ are computed using corrected $\widetilde{\boldsymbol{\tau}}$ as a function of $\mathbf{U_{10}}$ at float positions. Standard deviations of the averages of drag coefficients in three different wind speed bins ($|\mathbf{U_{10}}| = 27.5 \pm 2.5$, 35 ± 5, and > 40 m/s) are less than 0.5×10^{-3} (Figure 2).

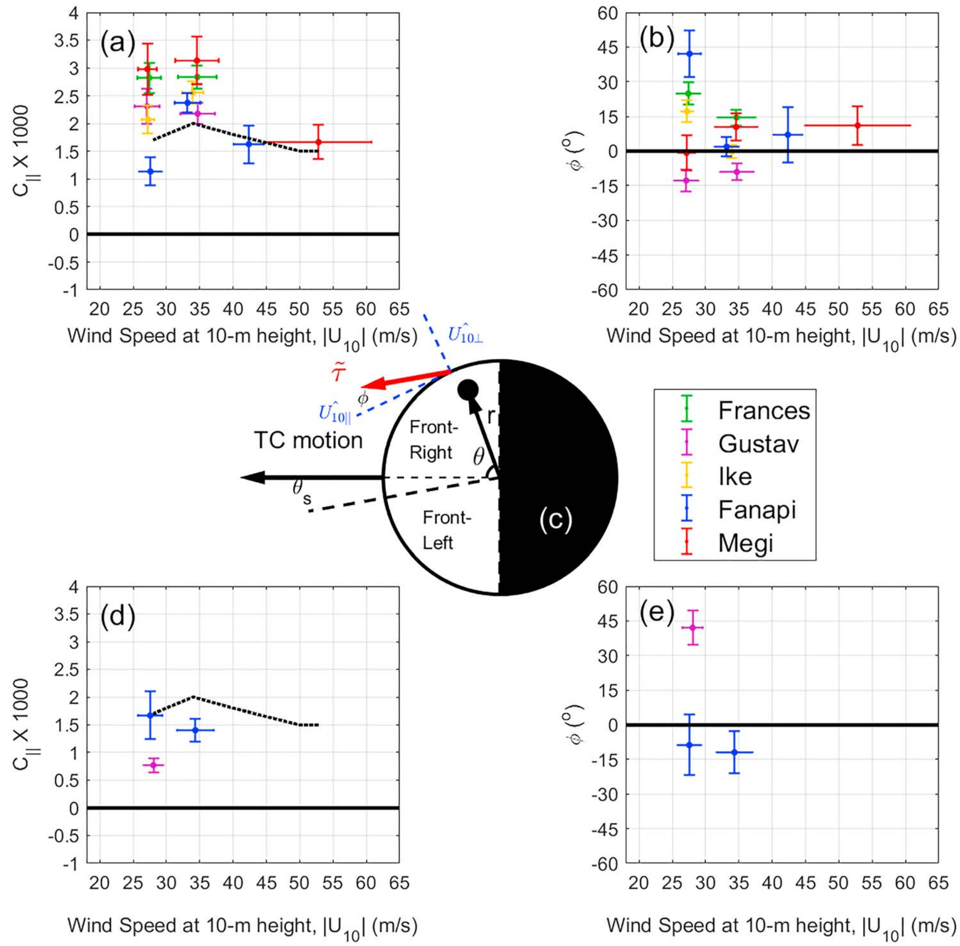

Figure 2. Estimates of adjusted downwind drag coefficient $\widetilde{C_{||}}$ (a and d) and the angle ϕ (b and e) between the surface wind stress $\tilde{\boldsymbol{\tau}}$ and wind $\mathbf{U_{10}}$ in five different tropical cyclones (colored lines), using the float measurements in the front-right (a and b) and front-left (d and e) sectors of tropical cyclones (c). The vertical error bars represent the standard deviations of $\widetilde{C_{||}}$ averages and ϕ, respectively, and the horizontal error bars represent the standard deviations of interpolated $|\mathbf{U_{10}}|$ at the float positions. The red arrow in (c) is an example of estimated surface wind stress $\tilde{\boldsymbol{\tau}}$ on the coordinates of crosswind $\widehat{\mathbf{U_{10}}}_{\perp}$ and downwind $\widehat{\mathbf{U_{10}}}_{||}$ directions (blue dashed lines in c). The boundary between two sectors is defined assuming $\theta_s = -10°$. For the positions of the floats, the azimuth $\theta > 0$ is clockwise from tropical cyclones' motion, and r the distance of floats to the tropical cyclone's eye. Black dashed lines are results using the Powell et al. (2003) drag coefficient.

5. Distribution of Drag Coefficients in Different Tropical Cyclone Sectors

Variations of drag coefficients are discussed in two sectors of tropical cyclones: front-right and front-left, divided by $\theta_s = -10^{o}$, where θ_s is the angle clockwise from the storms' translation direction (Figure 2c). The front-right sector includes estimates on the storm tracks (supporting information D).

At $|\mathbf{U_{10}}| = 25$–30 m/s, $\widetilde{C_{||}}$ varies between 1.1–2.9×10^{-3} in the front-right sector and is 0.8×10^{-3} (Gustav) and 1.7×10^{-3} (Fanapi) in the front-left sector (Figure 2). Higher $\widetilde{C_{||}}$ in the front-right sector agrees with previous model simulations (Chen et al., 2013; Moon et al., 2004) but is opposite to observations by Holthuijsen et al. (2012), presumably due to the presence of surface waves (supporting information C). Because of the consistent spatial distribution of $\widetilde{C_{||}}$ under two different storms (Gustav and Fanapi), we will discuss the $\widetilde{C_{||}}$ in the front-left sector of storms with those in the front-right sector together in the next section, though the measurements are fewer. At $|\mathbf{U_{10}}| = 30$–40 m/s, $\widetilde{C_{||}}$ in the front-right sector is 2.2–3.1×10^{-3}, higher than the peak C_d reported by Powell et al. (2003), ~2.0×10^{-3}. The scattering of $\widetilde{C_{||}}$ decreases at higher wind speeds. The estimates of $\widetilde{C_{||}}$ at $|\mathbf{U_{10}}| = 25$–40 m/s under both sectors of five tropical cyclones are least squares fitted as $\widetilde{C_{\parallel}} = (0.057|\mathbf{U_{10}}| + 0.42) \times 10^{-3}$ (not shown in the study) with the root-mean-square error (RMS) ~ 0.68×10^{-3}. The RMS is ~ 0.52×10^{-3} for the front-right sector alone. At $|\mathbf{U_{10}}| > 40$ m/s, $\widetilde{C_{\parallel}}$ in the front-right sector of Fanapi and Megi is saturated, ~1.6×10^{-3}, in good agreement with the saturation of C_d reported previously (Jarosz et al., 2007; Powell et al., 2003).

At $|\mathbf{U_{10}}| = 25$–30 m/s, the wind stress is clockwise from the wind $\mathbf{U_{10}}$ with $\phi = 15$–$40°$ in the front-right sector of Frances, Ike, and Fanapi. The $\widetilde{\boldsymbol{\tau}}$ is nearly aligned with the $\mathbf{U_{10}}$ in the front-right sector of Megi. The ϕ is ~ $-15°$ in the front-right sector of Gustav and 40° in the front-left sector. The ϕ in the front-right sector of storms varies from -15–$40°$ at $|\mathbf{U_{10}}| = 25$–30 m/s and becomes less scattered at $|\mathbf{U_{10}}| = 30$–40 m/s, $\pm 15°$. The decreasing scattering of ϕ at higher wind speed is similar with the trend of $\widetilde{C_{\parallel}}$. At wind speed $|\mathbf{U_{10}}| > 40$ m/s, $\widetilde{\boldsymbol{\tau}}$ is nearly aligned with the $\mathbf{U_{10}}$. The angle ϕ decreases with increasing wind speed.

6. Scaling Drag Coefficients Including Effects of Surface Waves

Many previous studies assume that drag coefficients depend on wind speed alone (e.g., Smith et al., 1992). However, reported drag coefficients scattered significantly from 1.5 to 4.5×10^{-3} at $|\mathbf{U_{10}}| = 25$–40 m/s (section 1), presumably due to effects of surface waves (e.g., Johnson et al., 1998; Smith et al., 1992). The wind forcing along the fetch of surface waves χ contributes most momentum transferred from the atmosphere into the ocean via wave breaking (Jones & Toba, 2012; Melville & Rapp, 1985).

Here, a nondimensional "effective" wind duration ζ is proposed for parameterizing the drag coefficients as

$$\zeta = \frac{gT}{|\mathbf{U_{10}}| \cos\psi} = \frac{g\left(\frac{\chi}{U_h}\right)}{|\mathbf{U_{10}}| \cos\psi} \tag{4}$$

where g is the gravity, T the duration of wind blowing along a fetch χ, and ψ the angle between dominant surface waves and $\mathbf{U_{10}}$. The rationale for these terms is as follows: Wind forcing with longer duration will generate surface waves with higher energy (Young, 1999). The cos ψ is added to adjust for the difference in wind and dominant wave directions. The T is defined as the time for a tropical cyclone to travel over a fetch χ at a translation speed U_h, that is, $T = \chi/U_h$. The fetch $\chi(r,\theta)$ is estimated using the expression in Hwang et al. (2016) (supporting information E) derived from data taken in Hurricane Bonnie. The value of ψ in degrees is computed as $\psi(°) = 30 + 6(U_h/U_{h0})$, where $U_{h0} = 1$ m/s in the front-left sector and as a constant ($\psi = 30°$) in the front-right sector, based on model simulation results in Moon et al. (2004). The spatial distribution of assumed ψ is consistent with the observed ψ in the previous studies (e.g., Black et al., 2007; Wright et al., 2001). The analysis on the effects of individual parameters in ζ to the parameterizations of drag coefficients is described in supporting information E.

At $|\mathbf{U_{10}}| = 25$–40 m/s, the $\widetilde{C_{\parallel}}$ is nearly constant at 2.5×10^{-3} for $\zeta < 8\times 10^3$ and decreases with increasing ζ (Figure 3a). Because ζ is inversely proportional to U_h in the front-right sector of storms, faster storms, such as Megi and Frances, tend to have higher $\widetilde{C_{\parallel}}$ than the slower storms, such as Ike and Fanapi (supporting information B). Though Gustav's U_h is nearly the same as Megi (~7.7 m/s), the dependence of ψ on the U_h results in the smallest value of $\widetilde{C_{\parallel}}$ in the front-left sector of Gustav, ~0.8×10^{-3}. Note that the difference of $\widetilde{C_{\parallel}}$ at $|\mathbf{U_{10}}| = 25$–30 m/s (Figure 2) between the front-left and front-right sectors of Fanapi (~0.5×10^{-3}) is smaller than that in Gustav (~1.5×10^{-3}), that is, the $\widetilde{C_{\parallel}}$ under Fanapi is more spatially homogeneous. The slow U_h of Fanapi (~3.8 m/s) may generate the homogeneous $\widetilde{C_{\parallel}}$, by balancing the opposite effects of wind forcing duration T and the magnitude of wind forcing $|\mathbf{U_{10}}|$ cosψ in the ζ.

The $\phi(\zeta)$ at $|\mathbf{U_{10}}| = 25$–40 m/s under five tropical cyclones has larger scattering than the $\widetilde{C_{\parallel}}(\zeta)$, but generally increases with increasing ζ. Most ϕ is within $\pm 15°$ at $\zeta < 12 \times 10^3$ and varies from -10 to ~40° at $\zeta > 12 \times 10^3$. Potter et al. (2015) report the estimated $\phi = 10$–$20°$ at $r > 5\ R_{\max}$ in the front-left sector of Typhoon Chaba 2010 (the cross-swell region in Holthuijsen et al., 2012), suggesting that the orientation of $\boldsymbol{\tau}$ may be altered by the swell. The orientation of $\boldsymbol{\tau}$ under faster storms may be less affected by the swell than that under slower storms, because the φ generally decreases with decreasing ζ.

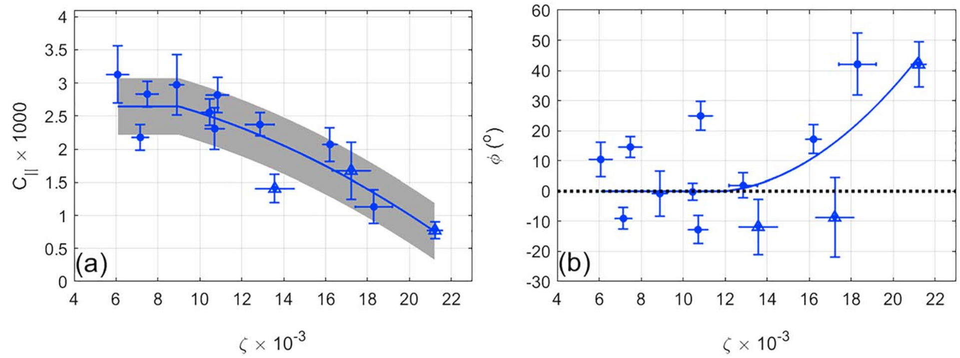

Figure 3. Dependence of adjusted downwind drag coefficient $\widetilde{C_{\|}}$ (a) and the angle ϕ between the surface wind stress $\tilde{\tau}$ and wind $\mathbf{U_{10}}$ (b) under five tropical cyclones at $|\mathbf{U_{10}}|$ = 25–40 m/s (front-right sector: dots; front-left sector: triangles) on the nondimensional effective wind duration ζ. The mean and standard deviation of the adjusted drag coefficient averages in each wind speed bin are used to generate 1,000 realizations in the stochastic simulation, assuming a normal distribution. The curve in (a) and (b) are the fitted parameterizations of $\widetilde{C_{\|}}$ and ϕ using all realizations, respectively. The bounds of gray area from the curve in (a) are the standard errors between individual drag coefficient estimates and fitted curve. See Figure 2 for the descriptions of vertical error bars. Horizontal error bars represent 1 standard deviation of ζ.

We parameterize all realizations of $\widetilde{C_{\|}}$ and ϕ in the front-right and front-left sectors of storms as a function of ζ (black lines in Figure 3), respectively. that is,

$$\widetilde{C_{\|}} \times 1000 = \begin{cases} 2.7 & ;\ \text{for } \dfrac{\zeta}{1000} = 6\text{--}9 \\ a_{\|}\left(\dfrac{\zeta}{1000}\right)^2 + b_{\|}\left(\dfrac{\zeta}{1000}\right) + c_{\|}; & \text{for } \dfrac{\zeta}{1000} = 9\text{--}21 \end{cases} \tag{5}$$

$$\phi(^\circ) = \begin{cases} 0 & ;\ \text{for } \dfrac{\zeta}{1000} = 6\text{--}12 \\ a_{\phi}\left(\dfrac{\zeta}{1000}\right)^2 + b_{\phi}\left(\dfrac{\zeta}{1000}\right) + c_{\phi}; & \text{for } \dfrac{\zeta}{1000} = 12\text{--}21 \end{cases} \tag{6}$$

The mean and standard deviation of the coefficients are $a_{\|} = (-5.2 \pm 0.2) \times 10^{-3}$, $b_{\|} = (3.8 \pm 5.5) \times 10^{-3}$, $c_{\|} = 3.05 \pm 0.03$, $a_{\phi} = 0.44 \pm 0.01$, $b_{\phi} = -9.70 \pm 0.19$, and $c_{\phi} = 52.45 \pm 0.16$. The RMS of $\widetilde{C_{\|}}(\zeta)$ and $\phi(\zeta)$ are about 0.35×10^{-3} and 14°, respectively. The RMS of $\widetilde{C_{\|}}(\zeta)$ improves the RMS of $\widetilde{C_{\|}}(|\mathbf{U_{10}}|) \sim 0.68 \times 10^{-3}$ under five storms, and those reported by the previous studies, from 1.5 to 4.5×10^{-3} at $|\mathbf{U_{10}}|$ = 25–40 m/s (section 1).

The new parameterization of $\widetilde{C_{\|}}(\zeta)$ is used to simulate the $C_d(|\mathbf{U_{10}}|)$ at $|\mathbf{U_{10}}|$ = 25–40 m/s under an idealized tropical cyclone (supporting information G) with different storm properties. The C_d is assumed the constant of 1.6×10^{-3} at $|\mathbf{U_{10}}|$ = 50 m/s (the average of Megi and Fanapi's $\widetilde{C_{\|}}$ in Figure 2), and linearly interpolated at $|\mathbf{U_{10}}|$ = 40–50 m/s. For a float deployed at 40 km to the right of storm's track, faster storms have higher C_d than slower storms (Figure 4a), assuming the storms with the constant $R_{\max}$ = 40 km but different U_h. The ocean model simulations using the C_d reported by Powell et al. (2003) may underestimate the current velocity at the assumed float positions if $U_h > 5$ m/s, and thereby the sea surface temperature cooling. Smaller storms tend to generate higher C_d than the larger storms (Figure 4b), but the effect of $R_{\max}$ to C_d is less than that of the U_h. The $\widetilde{C_{\|}}(\zeta)$ will benefit the future model studies on simulating the upper ocean response under different storms.

7. Discussion: Parameter ζ

Young (2003) discusses the importance of the time that surface waves remain in the intense wind region to the wave growth. We therefore define a "motion-forced" frequency f_r for surface waves when their group velocity c_g equals the storm translation speed U_h. For deep-water surface waves $k^*d > \pi$,

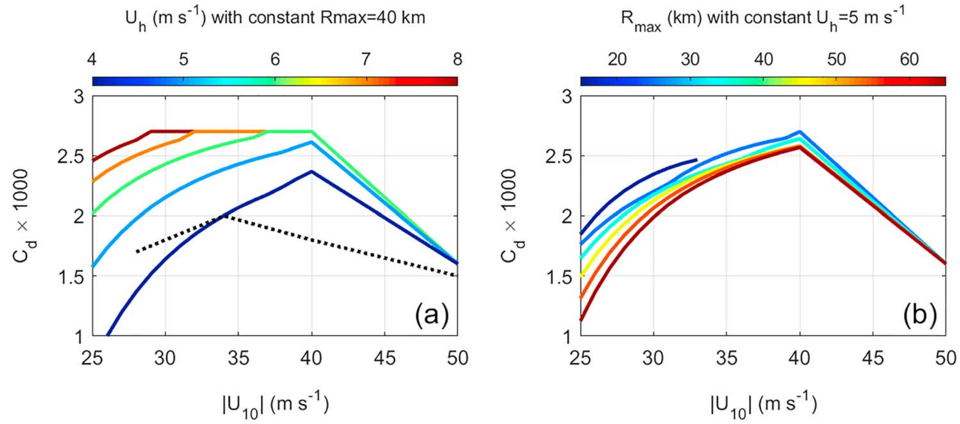

Figure 4. Simulated drag coefficient $C_d(|\mathbf{U_{10}}|)$ at 40 km to the front right of the track of an idealized tropical cyclone using the parameterization of $\widetilde{C_\parallel}(\zeta)$ in equation (5), assuming (a) different storm translation speed U_h (radius of maximum wind speed $R_{max} = 40$ km), and (b) different R_{max} ($U_h = 5$ m/s). Black dashed line in (a) is the C_d result reported by Powell et al. (2003).

$f_r = g/(4\pi c_g) = g/(4\pi U_h)$, where k is the wave number and d the ocean depth. These waves are forced continuously by the wind under a moving tropical cyclone. Because the f_r is inversely proportional to U_h, that is, $U_h \propto f_r^{-1}$, faster tropical cyclones (larger U_h) more effectively generate lower-frequency surface waves of a faster group velocity. The difference between c_g and U_h determines the time of wind forcing on surface waves in moving tropical cyclones (Young & Vinoth, 2013).

Because of the local equilibrium between the wind input and energy dissipation, the fetch χ of fetch-limited surface waves is inversely proportional to peak frequency f_p, that is, $\chi \propto f_p^{-1}$, under the constant wind speed (Fontaine, 2013). Therefore, the duration $T = \chi/U_h \propto f_r/f_p$. Lower f_r/f_p may imply higher wave energy S_η at f_r if $f_r/f_p > 1$, because most surface wave spectra under tropical cyclones have a single spectral peak at f_p (Hu & Chen, 2011; Young, 1998). Faster storms, such as Gustav, have the ratio of f_r/f_p closer to 1 than slower storms, such as Fanapi (supporting information F). Their wind $|\mathbf{U_{10}}|$ may "continuously" force surface waves at a more extended period such that surface waves contain higher energy S_η at the f_r (i.e., increase of wave height at f_r) and then result in wave breaking when the wave slope (the ratio of wave height to wavelength) at f_r exceeds 0.1 (Donelan et al., 2012). Most wave momentum is transferred by the breaking of high-frequency waves (small disturbances) instead of long waves (Jones & Toba, 2012). The transfer of wave momentum into the ocean current via wave breaking is proportional to the spectral level $S_\eta(f_r)$ (e.g., Donelan et al., 2012; Tolman & Chalikov, 1996). Stronger wave breaking may therefore occur under faster storms. The parameter T introduces a new concept for wave momentum transfer under a tropical cyclone moving at a speed of U_h.

This study uses the effective wind duration ζ to study the variability of drag coefficients. The ζ is parameterized by T, which may be regarded as an indicator of wave momentum transfer due to the wave breaking forced by moving tropical cyclones. The wind along the direction of dominant surface waves $|\mathbf{U_{10}}| \cos\psi$ in the ζ may be associated with the wind for inducing the wave breaking (Phillips, 1957; Miles, 1960; Donelan et al., 2012). According to the dependence of $\widetilde{C_\parallel}$ on the ζ in the front-right sector of storms (Figure 3a), faster storms may force more efficiently on surface waves with larger amplitude and result in stronger wave breaking, that is, more wave momentum transfer into the ocean current. The wave breaking under faster storms may therefore lead to higher drag coefficients than slower storms. The lower $\widetilde{C_\parallel}(\zeta)$ in the front-left sector of storms than in the front-right sector may be due to a greater angle of ψ, which results in less wind forcing for inducing wave breaking. The proposed parameter $\zeta \propto f_r/(f_p\, |\mathbf{U_{10}}| \cos\psi)$ is different from the previously proposed parameter wave age $c_p/|\mathbf{U_{10}}| \propto 1/(f_p|\mathbf{U_{10}}|)$ (Johnson et al., 1998), about the relative speed between wind and surface waves' phase speed c_p at the f_p.

The ζ presents the importance of wave breaking for the momentum transfer efficiency under the moving weather system, that is, $\widetilde{C_\parallel}(\zeta)$ under systems such as the propagating Madden-Julian oscillation may be estimated by using different definition of T in the future. Unfortunately, the wind distribution under tropical cyclones may make the $\widetilde{C_{\parallel}}(\zeta)$ in this study only applicable to systems as storms. Note that other tropical cyclones' properties, for example, the normalized distance of float positions to storms' eyes $r/R_{\max}$ (Hwang & Walsh, 2018), may affect the assumed χ and ψ, and thereby the $\widetilde{C_{\parallel}}(\zeta)$. We summarize several potential parameters that might be important to drag coefficients (supporting information F), and encourage further investigations, especially the parameterization of ϕ.

8. Conclusion

Nineteen EM-APEX floats were deployed from aircraft in five different tropical cyclones: Frances, Gustav, Ike, Fanapi, and Megi, to measure profiles of ocean current velocity, temperature, and salinity. The surface wind stress $\tilde{\boldsymbol{\tau}}$ is estimated by depth integrating the estimated wind-driven current in the linear momentum budget and used for computing the drag coefficients in the front-right and front-left sectors of tropical cyclones.

At $|\mathbf{U_{10}}| = 25$–40 m/s, the downwind drag coefficient $\widetilde{C_{\parallel}}$ in the front-right sector of tropical cyclones, 1.1–3.1 $\times 10^{-3}$, is mostly higher than that in the front-left sector of Gustav and Fanapi, 0.8 $\times 10^{-3}$ and 1.7 $\times 10^{-3}$, respectively. The peak $\widetilde{C_{\parallel}}$ is found at $|\mathbf{U_{10}}| = 30$–40 m/s. The $\widetilde{C_{\parallel}}$ in Fanapi and Megi is saturated at $|\mathbf{U_{10}}| > 40$ m/s, ~1.6 $\times 10^{-3}$, in good agreement with the C_d reported by Powell et al. (2003). The angle ϕ in the front-right sector of tropical cyclones is −15–40° at $|\mathbf{U_{10}}| = 25$–30 m/s, and the scatter of ϕ decreases with increasing $|\mathbf{U_{10}}|$.

The estimates of drag coefficients at $|\mathbf{U_{10}}| = 25$–40 m/s are parameterized for the first time as a function of the effective wind duration ζ (equations (5) and (6)), associated with the wind forcing, storm translation speed, and fetch. Parameterization based on these factors fits the variations in the $\widetilde{C_{\parallel}}$ of 0.8–3.1 $\times 10^{-3}$ to a RMS of 0.35 $\times 10^{-3}$, better than the RMS of conventional parameterization of $\widetilde{C_{\parallel}}(|\mathbf{U_{10}}|)$ ~ 0.68 $\times 10^{-3}$. The $\varphi(\zeta)$ has a RMS ~ 14°, presumably due to other factors, such as the misalignment between wind and swell. The $\widetilde{C_{\parallel}}$ in the front-right sector of tropical cyclones decreases with slower U_h, implying less transfer of wave momentum under slower storms. The $\widetilde{C_{\parallel}}$ in the front-left sector of tropical cyclones is lower than in the front-right sector, which may be resulted from a greater angle between the wind and waves. The U_h of tropical cyclones may alter the surface wind stress $\boldsymbol{\tau}$ by affecting not only the time for surface waves staying in the moving tropical cyclone but also the wind forcing on the dominant surface waves.

This study presents a new data-based parameterization of drag coefficients at $|\mathbf{U_{10}}| = 25$–40 m/s by considering the interaction between surface waves and wind forcing under moving tropical cyclones. Including the concept of wave momentum transfer in this parameterization emphasizes the importance of tropical cyclone-wave-ocean interactions, in good agreement with the previous model studies (e.g., Chen et al., 2013; Reichl et al., 2014). These results are important and useful to guide future model studies on the oceanic thermal and momentum responses to tropical cyclones, especially the maximum cooling on the right of tropical cyclone tracks. Because ζ can be a predictor of wave breaking under moving weather systems, $\widetilde{C_{\parallel}}(\zeta)$ may be estimated in other moving weather systems in the future, such as the propagating Madden-Julian oscillation.

Acknowledgments
The processed data for the drag coefficient analysis in this study is summarized in the tables of the supporting information (SI). Further analysis on the parameters of drag coefficient parameterization using the SI is encouraged. The authors appreciate the Office of Naval Research Physical Oceanography Program (N00014-08-1-0560, N00014-08-1-0577, N00014-10-1-0313, N00014-11-1-0375, and N00014-14-1-0360) for their support, AOML/HRD/NOAA for providing SFMR measurements under Frances, Gustav and Ike at http://www.aoml.noaa.gov/hrd/data_sub/sfmr.html, UCAR/NCAR for the dropsondes measurements at https://www.eol.ucar.edu/observing_facilities/avaps-dropsonde-system, and the 53rd Weather Reconnaissance Squadron for deploying the EM-APEX floats. The authors would like to dedicate this paper to Theresa Paluszkiewicz of ONR for her vision in supporting innovative ocean experiments and technology and, in particular, the EM-APEX profiler that forms the basis of this work. The authors extend special thanks to J. Carlson and J. Dunlap for designing and building the EM sensor systems on the EM-APEX float, J. Thomson in APL for checking the explanation of high drag coefficients due to the wave breaking.

References

Balaguru, K., Foltz, G. R., Leung, L. R., D'Asaro, E., Emanuel, K. A., Liu, H., & Zedler, S. E. (2015). Dynamic potential intensity: An improved representation of the ocean's impact on tropical cyclones. *Geophysical Research Letters*, *42*, 6739–6746. https://doi.org/10.1002/2015GL064822

Black, P. G., D'Asaro, E., Sanford, T. B., Drennan, W. M., Zhang, J. A., French, J. R., et al. (2007). Air–sea exchange in hurricanes: Synthesis of observations from the coupled boundary layer air-sea transfer experiment. *Bulletin of the American Meteorological Society*, *88*(3), 357–374. https://doi.org/10.1175/BAMS-88-3-357

Bryant, K. M., & Akbar, M. (2016). An exploration of wind stress calculation techniques in hurricane storm surge modeling. *Journal of Marine Science and Engineering*, *4*(3), 58. https://doi.org/10.3390/jmse4030058

Chen, S. S., Zhao, W., Donelan, M. A., & Tolman, H. L. (2013). Directional wind-wave coupling in fully coupled atmosphere-wave-ocean models: Results from CBLAST-hurricane. *Journal of the Atmospheric Sciences*, *70*(10), 3198–3215. https://doi.org/10.1175/JAS-D-12-0157.1

D'Asaro, E. A., Black, P. G., Centurioni, L. R., Chang, Y. T., Chen, S. S., Foster, R. C., et al. (2014). Impact of typhoons on the ocean in the Pacific. *Bulletin of the American Meteorological Society*, *95*(9), 1405–1418. https://doi.org/10.1175/BAMS-D-12-00104.1

Donelan, M. A., Curcic, M., Chen, S. S., & Magnusson, A. K. (2012). Modeling waves and wind stress. *Journal of Geophysical Research*, *117*, C00J23. https://doi.org/10.1029/2011JC007787

Donelan, M. A., Haus, B. K., Reul, N., Plant, W. J., Stiassnie, M., Graber, H. C., et al. (2004). On the limiting aerodynamic roughness of the ocean in very strong winds. *Geophysical Research Letters*, *31*, L18306. https://doi.org/10.1029/2004GL019460

Edson, J. B., Jampana, V., Weller, R. A., Bigorre, S. P., Plueddemann, A. J., Fairall, C. W., et al. (2013). On the exchange of momentum over the open ocean. *Journal of Physical Oceanography*, *43*(8), 1589–1610. https://doi.org/10.1175/JPO-D-12-0173.1

Emanuel, K. A. (1995). Sensitivity of tropical cyclones to surface exchange coefficients and a revised steady-state model incorporating eye dynamics. *Journal of the Atmospheric Sciences*, *52*(22), 3969–3976. https://doi.org/10.1175/1520-0469(1995)052<3969:SOTCTS>2.0.CO;2

Fontaine, E. (2013). A theoretical explanation of the fetch- and duration-limited laws. *Journal of Physical Oceanography*, *43*(2), 233–247. https://doi.org/10.1175/JPO-D-11-0190.1

Holthuijsen, L. H., Powell, M. D., & Pietrzak, J. D. (2012). Wind and waves in extreme hurricanes. *Journal of Geophysical Research*, *117*, C09003. https://doi.org/10.1029/2012JC007983

Hsu, J.-Y., Lien, R.-C., D'Asaro, E. A., & Sanford, T. B. (2017). Estimates of surface wind stress and drag coefficients in typhoon Megi. *Journal of Physical Oceanography*, *47*(3), 545–565. https://doi.org/10.1175/jpo-d-16-0069.1

Hu, K., & Chen, Q. (2011). Directional spectra of hurricane-generated waves in the Gulf of Mexico. *Geophysical Research Letters*, *38*, L19608. https://doi.org/10.1029/2011GL049145

Hwang, P. A. (2016). Fetch- and duration-limited nature of surface wave growth inside tropical cyclones. With applications to air–sea exchange and remote sensing. *Journal of Physical Oceanography*, *46*(1), 41–56. https://doi.org/10.1175/JPO-D-15-0173.1

Hwang, P. A., Li, X., Zhang, B., & Walsh, E. (2016). Fetch-limited surface wave growth inside tropical cyclones and hurricane wind speed retrieval, Geoscience and Remote Sensing Symposium (IGARSS). IEEE International, 10–15 July 2016.

Hwang, P. A., & Walsh, E. J. (2018). Propagation directions of ocean surface waves inside tropical cyclones. *Journal of Physical Oceanography*, *48*(7), 1495–1511. https://doi.org/10.1175/JPO-D-18-0015.1

Jarosz, E., Mitchell, D. A., Wang, D. W., & Teague, W. J. (2007). Bottom-up determination of air-sea momentum exchange under a major tropical cyclone. *Science*, *315*(5819), 1707–1709. https://doi.org/10.1126/science.1136466

Johnson, H. K., Højstrup, J., Vested, H. J., & Larsen, S. E. (1998). On the dependence of sea surface roughness on wind waves. *Journal of Physical Oceanography*, *28*(9), 1702–1716. https://doi.org/10.1175/1520-0485(1998)028<1702:OTDOSS>2.0.CO;2

Jones, I. S. F., & Toba, Y. (2012). *Wind stress over the ocean*. Cambridge: Cambridge University Press. https://doi.org/10.1017/CBO9780511552076

Large, W. G., & Pond, S. (1981). Open ocean momentum flux measurements in moderate to strong winds. *Journal of Physical Oceanography*, *11*(3), 324–336. https://doi.org/10.1175/1520-0485(1981)011<0324:OOMFMI>2.0.CO;2

Melville, W. K., & Rapp, R. J. (1985). Momentum flux in breaking waves. *Nature*, *317*(6037), 514–516. https://doi.org/10.1038/317514a0

Miles, J. W. (1960). On the generation of surface waves by turbulent shear flows. *Journal of Fluid Mechanics*, *7*(03), 469–478. https://doi.org/10.1017/S0022112060000220

Moon, I.-J., Ginis, I., & Hara, T. (2004). Effect of surface waves on air–sea momentum exchange. Part II: Behavior of drag coefficient under tropical cyclones. *Journal of the Atmospheric Sciences*, *61*(19), 2334–2348. https://doi.org/10.1175/1520-0469(2004)061<2334:EOSWOA>2.0.CO;2

Phillips, O. M. (1957). On the generation of waves by turbulent wind. *Journal of Fluid Mechanics*, *2*(05), 417–445. https://doi.org/10.1017/S0022112057000233

Potter, H., Collins, C. O. III, Drennan, W. M., & Graber, H. C. (2015). Observations of wind stress direction during typhoon Chaba (2010). *Geophysical Research Letters*, *42*, 9898–9905. https://doi.org/10.1002/2015GL065173

Powell, M. D., Vickery, P. J., & Reinhold, T. A. (2003). Reduced drag coefficient for high wind speeds in tropical cyclones. *Nature*, *422*(6929), 279–283. https://doi.org/10.1038/Nature01481

Price, J. F., Sanford, T. B., & Forristall, G. Z. (1994). Forced stage response to a moving hurricane. *Journal of Physical Oceanography*, *24*(2), 233–260. https://doi.org/10.1175/1520-0485(1994)024<0233:FSRTAM>2.0.CO;2

Rabe, T. J., Kukulka, T., Ginis, I., Hara, T., Reichl, B. G., D'Asaro, E. A., et al. (2015). Langmuir turbulence under hurricane Gustav (2008). *Journal of Physical Oceanography*, *45*(3), 657–677. https://doi.org/10.1175/JPO-D-14-0030.1

Reichl, B. G., Hara, T., & Ginis, I. (2014). Sea state dependence of the wind stress over the ocean under hurricane winds. *Journal of Geophysical Research: Oceans*, *119*, 30–51. https://doi.org/10.1002/2013JC009289

Sanford, T. B., Dunlap, J. H., Carlson, J. A., Webb, D. C., & Girton, J. B. (2005). Autonomous velocity and density profiler: EM-APEX. Paper presented at the current measurement technology, 2005, Proceedings of the IEEE/OES Eighth Working Conference on, 28–29 June 2005. IEEE Cat. No. 05CH37650

Sanford, T. B., Price, J. F., & Girton, J. B. (2011). Upper-ocean response to Hurricane Frances (2004) observed by profiling EM-APEX floats*. *Journal of Physical Oceanography*, *41*(6), 1041–1056. https://doi.org/10.1175/2010JPO4313.1

Smith, S. D., Anderson, R. J., Oost, W. A., Kraan, C., Maat, N., de Cosmo, J., et al. (1992). Sea surface wind stress and drag coefficients: The hexos results. *Boundary-Layer Meteorology*, *60*(1-2), 109–142. https://doi.org/10.1007/BF00122064

Takagaki, N., Komori, S., Suzuki, N., Iwano, K., Kuramoto, T., Shimada, S., et al. (2012). Strong correlation between the drag coefficient and the shape of the wind sea spectrum over a broad range of wind speeds. *Geophysical Research Letters*, *39*, 23604. https://doi.org/10.1029/2012GL053988

Tolman, H. L., & Chalikov, D. (1996). Source terms in a third-generation wind wave model. *Journal of Physical Oceanography*, *26*(11), 2497–2518. https://doi.org/10.1175/1520-0485(1996)026<2497:STIATG>2.0.CO;2

Wright, C. W., Walsh, E. J., Vandemark, D., Krabill, W. B., Garcia, A. W., Houston, S. H., et al. (2001). Hurricane directional wave spectrum spatial variation in the open ocean. *Journal of Physical Oceanography*, *31*(8), 2472–2488. https://doi.org/10.1175/1520-0485(2001)031<2472:HDWSSV>2.0.CO;2

Young, I. R. (1998). Observations of the spectra of hurricane generated waves. *Ocean Engineering*, *25*(4-5), 261–276. https://doi.org/10.1016/S0029-8018(97)00011-5

Young, I. R. (1999). *Wind generated ocean waves* (Vol. 2, pp. 12–160). Amsterdam: Elsevier.

Young, I. R. (2003). A review of the sea state generated by hurricanes. *Marine Structures*, *16*(3), 201–218. https://doi.org/10.1016/S0951-8339(02)00054-0

Young, I. R., & Vinoth, J. (2013). An 'extended fetch' model for the spatial distribution of tropical cyclone wind-waves as observed by altimeter. *Ocean Engineering*, *70*, 14–24. https://doi.org/10.1016/j.oceaneng.2013.05.015

References From the Supporting Information

Holland, G. J. (1980). An analytic model of the wind and pressure profiles in hurricanes. *Monthly Weather Review*, *108*(8), 1212–1218. https://doi.org/10.1175/1520-0493(1980)108<1212:AAMOTW>2.0.CO;2

Hsu, J.-Y., Lien, R.-C., D'Asaro, E. A., & Sanford, T. B. (2018). Estimates of surface waves using subsurface EM-APEX floats under typhoon Fanapi 2010. *Journal of Atmospheric and Oceanic Technology*, *35*(5), 1053–1075. https://doi.org/10.1175/JTECH-D-17-0121.1

Hwang, P. A., Fan, Y., Ocampo-Torres, F. J., & García-Nava, H. (2017). Ocean surface wave spectra inside tropical cyclones. *Journal of Physical Oceanography*, *47*(10), 2393–2417. https://doi.org/10.1175/jpo-d-17-0066.1

Sullivan, P. P., Romero, L., McWilliams, J. C., & Melville, W. K. (2012). Transient evolution of Langmuir turbulence in ocean boundary layers driven by hurricane winds and waves. *Journal of Physical Oceanography*, *42*(11), 1959–1980. https://doi.org/10.1175/JPO-D-12-025.1

UCAR/NCAR (2016). Earth observing laboratory, 1993-present. NCAR Airborne Vertical Atmospheric Profiling System (AVAPS). https://doi.org/10.5065/D66W9848, https://www.eol.ucar.edu/observing_facilities/avaps-dropsonde-system

Uhlhorn, E. W., & Black, P. G. (2003). Verification of remotely sensed sea surface winds in hurricanes. *Journal of Atmospheric and Oceanic Technology*, *20*(1), 99–116. https://doi.org/10.1175/1520-0426(2003)020<0099:VORSSS>2.0.CO;2

Uhlhorn, E. W., Black, P. G., Franklin, J. L., Goodberlet, M., Carswell, J., & Goldstein, A. S. (2007). Hurricane surface wind measurements from an operational stepped frequency microwave radiometer. *Monthly Weather Review*, *9*, 3070–3085.

Zhang, J. A., & Uhlhorn, E. W. (2012). Hurricane sea surface inflow angle and an observation-based parametric model. *Monthly Weather Review*, *140*(11), 3587–3605. https://doi.org/10.1175/MWR-D-11-00339.1